PERGAMON

Available online at www.sciencedirect.com
SCIENCE DIRECT®

International Journal of Heat and Mass Transfer 46 (2003) 2727–2735

International Journal of HEAT and MASS TRANSFER

www.elsevier.com/locate/ijhmt

Heat exchange between two coupled fixed beds by fluid flow

J.J. Saastamoinen *

VTT Processes, Koivurannantie, P.O. Box 1603, 40101 Jyväskylä, Finland

Received 9 March 2001; received in revised form 20 January 2003

Abstract

Heat exchange by forced fluid flow between two coupled fixed beds containing solids can be used to recover heat from hot products to cool input in many industrial processes. The heat exchange between the fixed beds is studied. Analytical solutions for the transient fluid and solid temperature distributions and heat recovery effectiveness are derived. The intra-particle transient temperature distributions are accounted for in the more accurate analysis and the results are compared to lumped analysis. It is shown that the heat recovery effectiveness reaches maximum at certain optimum time instant at which the fluid circulation should be stopped. Damping of cyclic oscillations in fluid temperature or concentration is considered and analytical solution for the damper is presented.

1. Introduction

The heat transfer phenomena in the single fixed bed of solids [1–11] or analogous phenomena [12] has been studied extensively. Fluid circulation between two fixed beds can be used to recover heat from hot products arranged in one fixed bed to heat the cool input in another fixed bed in industrial batch heating processes. Then heat recovery is applied to successive batch heating processes. It is possible to use the heat of the previous batch to preheat the next batch. Possible applications are in metal, glass, brick, coke, ceramics and food industries. The principle is illustrated in Fig. 1. For example, the elements of the two batches in Fig. 1 could be food in packed tins or glass in a heating process to destroy microbes by heating. A very illustrative example is a batch process for boiling of eggs from which the heat is partially recovered for the preheating of the next batch. After the fluid circulation between the beds is started, the fluid (gas or liquid) carries heat from the hot product container to heat the solids in the cool container. The fluid from the cool bed cools the hot bed. If the circulation is continued long time, the temperatures of the containers will smooth and be equal. This situation corresponds to the heat recovery efficiency 0.5. However, it is more favourable to stop the circulation at certain optimum time instant in order to maximise the heat recovery efficiency. After that the cooled products are removed, and new cool input can be placed in the container. The preheated input is finally heated with auxiliary energy to the final process temperature.

2. Preliminary discussion on single fixed bed

2.1. Governing equations

At first a single bed of solids is considered. Usually it is assumed that the thermal resistance of the solids can be neglected or that the conduction is lumped into effective thermal conductance [1–7], but also intra-particle conduction effect has been considered [8] by a numerical model. This will be studied here analytically. The heat conduction and storage inside the single solid bed elements is described by the Fourier equation and convective boundary condition

$$\frac{\partial T_p}{\partial t} = a_p \nabla^2 T_p, \quad h(T_f - T_s) = \lambda_p \left(\frac{\partial T_p}{\partial x}\right)_s \tag{1}$$

* Tel.: +358-12-672-547; fax: +358-14-672-597/596.
E-mail address: jaakko.saastamoinen@vtt.fi (J.J. Saastamoinen).

0017-9310/03/$ - see front matter © 2003 Elsevier Science Ltd. All rights reserved.
doi:10.1016/S0017-9310(03)00046-2

Nomenclature

a	thermal diffusivity of solid, $a = \lambda_p/(\rho_p c_p)$ [$m^2\,s^{-1}$]
Bi	Biot number, $Bi = hR/\lambda$
C	heat capacity, $C = cm$ [$J\,K^{-1}$]
$\dot{C}$	heat capacity flow rate, $\dot{C} = c_f \dot{m}_f$ [$W\,K^{-1}$]
c	specific heat [$J\,kg^{-1}\,K^{-1}$]
Fo	Fourier number, dimensionless time, $Fo = at/R^2$
h	heat transfer coefficient [$W\,m^{-2}\,K^{-1}$]
$\Im$	imaginary part
i	imaginary unit, $i = \sqrt{-1}$
L	length [m]
m	mass [kg]
$\dot{m}$	mass flow rate [$kg\,s^{-1}$]
p	Laplace transform variable (transform with respect to space co-ordinate)
R	characteristic length of an element, half thickness of a plate, radius of a cylinder or a sphere
$\Re$	real part
S	heat transfer area [m^2]
s	Laplace transform variable (transform with respect to time)
T	temperature [K]
t	time [s]
x	co-ordinate normal to the surface of the element [m]
y	co-ordinate along gas flow [m]

Greek symbols

α	mixing ratio
ε	thermal effectiveness of heat recovery
ϕ	shape coefficient for internal conduction, $\phi = 1/(2\Gamma + 6)$
Γ	element shape factor, 0 for a plate, 1 for a cylinder, 2 for a sphere γ
γ	ratio of heat capacities, $\gamma = C_f/C_p$
ς	dimensionless co-ordinate normal to the element surface, $\varsigma = x/R$
η	dimensionless time, $\eta = h_e St/C_p$
ϑ	dimensionless temperature of fluid, $\vartheta = (T_f - T_{p0})/(T_{f0} - T_{p0})$ for a single bed, $\vartheta = (T_f - T_{p,1})/(T_{p,2} - T_{p,1})$ for two beds coupled in series
θ	dimensionless temperature of solid, $\theta = (T_p - T_{p0})/(T_{f0} - T_{p0})$ for a single bed, $\theta = (T_p - T_{p,1})/(T_{p,1} - T_{p,2})$ for two beds coupled in series
Λ	dimensionless length, dimensionless heat transfer area, $\Lambda = hS/\dot{C}_f$
λ	thermal conductivity [$W\,m^{-1}\,K^{-1}$]
ξ	dimensionless co-ordinate along the fluid flow, $\xi = (hS/\dot{C})y/L$
ω	dimensionless frequency with respect to time ($\omega = 2\pi/Fo_c$) or space ($\omega = \pi/\Lambda$) co-ordinate

Subscripts

0	initial, inlet
1	bed with cooler initial temperature
2	bed with hotter initial temperature
a	average
c	cycle
e	effective, divided by $1 + 2\phi Bi$
f	fluid
p	solid
s	surface
t	total

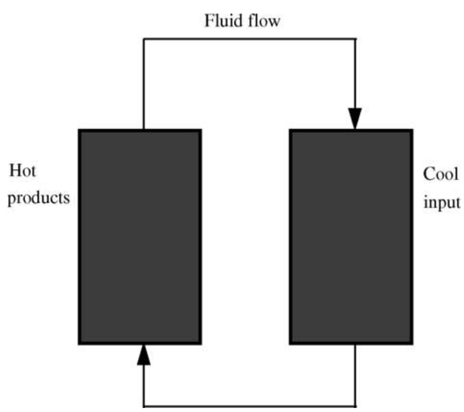

Fig. 1. Schematic of two coupled fixed beds.

The average heat transfer coefficient around the bed element surface is applied. The fixed bed is assumed to be ideally insulated and the flow across the bed distributed evenly. Then there are no temperature differences normal to the flow direction. Amundson [9] studied the non-insulated fixed bed with temperature distribution across the flow. The effect of axial conduction in the solids has been considered for a bed consisting of continuous plates [10] and in fluid for a bed of spherical particles [11]. The heat conduction in the solid or gas in the flow direction is considered insignificant compared to the convective heat flow in the analysis. Constant solid and fluid properties are assumed. The element characteristic size that determines the heating rate of the element is assumed to be small compared to the bed length and can be considered differential. Then the heat transfer in the fluid is described by

$$-\dot{C}_{\rm f}\frac{\partial T_{\rm f}}{\partial y}-(C_{\rm f}/L)\frac{\partial T_{\rm f}}{\partial t}=h(S/L)(T_{\rm f}-T_{\rm s})=(C_{\rm p}/L)\frac{{\rm d}T_{\rm pa}}{{\rm d}t} \tag{2}$$

The first term on the left-hand side accounts for the heat carried with the fluid flow and the second is due to heat storage in the fluid. This equals to the convective heat exchange between the fluid and the surface of the solids, which is also equal to the energy storage in the solids. The heat transported by conduction and mixing in the flow direction is assumed to be insignificant compared to the forced convection flow. The initial conditions of the bed material and the fluid inside the bed are $T_{\rm p}=T_{\rm f}=T_0$.

Eqs. (1) and (2) can be presented in dimensionless form for one-dimensional cases

$$\begin{aligned}&\frac{\partial\theta}{\partial Fo}=\frac{1}{\varsigma^{\Gamma}}\frac{\partial}{\partial\varsigma}\left(\varsigma^{\Gamma}\frac{\partial\theta}{\partial\varsigma}\right),\\&\vartheta-\theta_{\rm s}=\frac{1}{Bi}\left(\frac{\partial\theta}{\partial\varsigma}\right)_{\rm s}=-\frac{\partial\vartheta}{\partial\xi}-\frac{\gamma}{Bi(1+\Gamma)}\\&\frac{\partial\vartheta}{\partial Fo}=\frac{1}{Bi(1+\Gamma)}\frac{{\rm d}\theta_{\rm a}}{{\rm d}Fo}\end{aligned} \tag{3}$$

2.2. Exact solutions for step response and cyclic operation

We apply the Laplace transform

$$\bar{f}(s)=\int_0^\infty {\rm e}^{-sFo}f(Fo)\,{\rm d}Fo \tag{4}$$

Eqs. (3) are transformed into

$$\begin{aligned}&s\bar\theta=\frac{1}{\varsigma^{\Gamma}}\frac{\rm d}{{\rm d}x}\left(\frac{1}{\varsigma^{\Gamma}}\frac{{\rm d}\bar\theta}{{\rm d}\varsigma}\right),\quad Bi(\bar\vartheta-\bar\theta_{\rm s})=\left(\frac{{\rm d}\bar\theta_{\rm s}}{{\rm d}\varsigma}\right)_{\rm s},\\&-\frac{\partial\bar\vartheta}{\partial\xi}-\frac{\gamma s\bar\vartheta}{Bi(1+\Gamma)}=\bar\vartheta-\bar\theta_{\rm s}=\frac{s\bar\theta_{\rm a}}{Bi(1+\Gamma)}\end{aligned} \tag{5}$$

The solution of the transformed solid temperature can be presented in the form

$$\begin{aligned}&\bar\theta=\bar\theta_{\rm s}\bar{m}(\varsigma,s),\\&\bar{m}(\varsigma,s)=\varsigma^{-(\Gamma-1)/2}J_{(\Gamma-1)/2}({\rm i}\varsigma\sqrt{s})/J_{(\Gamma-1)/2}({\rm i}\sqrt{s})\end{aligned} \tag{6}$$

where J is Bessel function of the first kind. The transformed element surface temperature can be related to the transformed fluid temperature

$$\bar\theta_{\rm s}=[1-\bar{h}(s)]\bar\vartheta \tag{7}$$

where $\bar{h}(s)=\bar{m}'(1,s)/[Bi+\bar{m}'(1,s)]$, $\bar{m}'(1,s)=-{\rm i}\sqrt{s}J_{(\Gamma+1)/2}({\rm i}\sqrt{s})/J_{(\Gamma-1)/2}({\rm i}\sqrt{s})$.

The function $\bar{h}(s)$ can be determined analytically also to some regular shaped two- and three-dimensional elements. In this case the surface temperature is not constant and average value is applied for $\theta_{\rm s}$. The solution of the differential equation for the fluid is readily found. The transformed fluid temperature and average element temperature are

$$\begin{aligned}&\bar\vartheta=\bar\vartheta_0{\rm e}^{-\bar{h}_*(s)\xi},\quad \bar\theta_{\rm a}=\bar\vartheta_0 Bi(1+\Gamma){\rm e}^{-\bar{h}_*(s)\xi}\bar{h}(s)/s,\\&\bar{h}_*(s)=\bar{h}(s)+\gamma s/[Bi(1+\Gamma)]\end{aligned} \tag{8}$$

The responses of the fluid temperature to a step change from 0 to 1 in the fluid inlet temperature, $\vartheta(\xi=0,Fo)=1$, when $\vartheta(\xi,0)=\theta(\xi,\varsigma,Fo=0)=0$, is found from the frequency response

$$\vartheta=1-\frac{2}{\pi}\int_0^\infty {\rm e}^{-\Re[\bar{h}({\rm i}\omega)]\xi}\sin\{\Im[\bar{h}({\rm i}\omega)]\xi\}\cos[\omega\{Fo-\gamma\xi/(Bi(1+\Gamma)\}]\frac{{\rm d}\omega}{\omega} \tag{9}$$

The corresponding temperature of the solid can also readily be found. In steady cyclic state, when the inlet fluid temperature varies as $\vartheta=\sin(\omega Fo)$, the response is

$$\vartheta=\exp\{-\Re[\bar{h}({\rm i}\omega)]\xi\}\sin\{\omega Fo-\Im[\bar{h}({\rm i}\omega)]\xi-\gamma\omega\xi/[Bi(1+\Gamma)]\} \tag{10}$$

2.3. Approximate solution for step response

It is difficult to apply the formal solution, Eq. (9). An approximate solution with a good accuracy after the initial stage is derived in the following. The well-known solution of the average element temperature, when the temperature of the fluid surrounding the element changes stepwise

$$\theta_{\rm a}=\vartheta\left(1-\sum_{n=1}^{\infty}K_n{\rm e}^{-\mu_n^2 Fo}\right) \tag{11}$$

This solution is presented in many books on heat transfer [13,14]. The eigenvalues are obtained as roots μ_n of the transcendental equation

$$\mu_n J_{(\Gamma+1)/2}(\mu_n)=BiJ_{(\Gamma-1)/2}(\mu_n) \tag{12}$$

The coefficients K_n are

$$K_n=2(1+\Gamma)Bi^2/\{\mu_n^2[\mu_n^2+Bi(1-\Gamma+Bi)]\} \tag{13}$$

Analytical solutions for the coefficients K_n and the eigenvalues for regular two- and three-dimensional element shapes (finite cylinders, cubes and so on) can also readily be derived. By applying the Laplace transform it can be seen the function $\bar{h}(s)$ defined by Eq. (7) can also be expressed as the series

$$\begin{aligned}\bar{h}(s)&=\frac{1}{Bi(1+\Gamma)}\sum_{n=1}^{\infty}K_n\mu_n^2\frac{s}{s+\mu_n^2}\\&=\frac{1}{Bi(1+\Gamma)}\left(K_1\mu_1^2\frac{s}{s+\mu_1^2}+(1-K_1)s+H(s)\right)\end{aligned} \tag{14}$$

where $H(s)=\sum_{n=2}^{\infty}K_n\sum_{k=1}^{\infty}(-s/\mu_n^2)^k$, since $\sum_{n=2}^{\infty}K_n=1-K_1$.

It is seen that the correction term $H(s)$ in Eq. (14) is small, since the summation in the series is started not until $n = 2$. In addition, small values of transform variable s correspond to moderate and large values of time. In the inversion, the correction term $H(s)$ is assumed to be zero. Only the first coefficient K_1 and eigenvalue μ_1 are required in practical calculations. These can be determined numerically for irregular element shapes. Now the step response is considered and $\bar{\vartheta}_0 = 1/s$. We apply the inverse Laplace transforms, Eq. (A.2), see Appendix A. The fluid and average solid temperatures become

$$\vartheta = G(\xi_*, Fo_*)U(Fo_*),$$
$$\theta_a = \{K_1[1 - G(Fo_*, \xi_*)] + (1 - K_1)G(\xi_*, Fo_*)\}U(Fo_*) \quad (15)$$

where $\xi_* = K_1\mu_1^2\xi/[Bi(1+\Gamma)]$, $Fo_* = \mu_1^2\{Fo - (1 - K_1 + \gamma)\xi/[Bi(1 + \Gamma)]\}$ and U is the Heaviside's unit step function, $U(x) = 1$ when $x \geqslant 0$ and $U(x) = 0$ when $x < 0$.

3. Two coupled fixed beds

Two similar beds ($\Lambda_1 = \Lambda_2$) are coupled together with a fluid flow between them. It is assumed that no heat losses take place in the channels connecting the fixed beds, but the theory can readily be generalised to account for heat losses or indirect heat exchange via a heat exchanger. It is assumed that the containers connected in series are similar having equally shaped and sized elements and equal heat transfer coefficients.

The initial temperatures of the containers are constants. The temperature scale is chosen so that

$$\vartheta(\xi_1, 0) = \theta(\xi_1, \varsigma_1, 0) = 0, \quad \vartheta(\xi_2, 0) = \theta(\xi_2, \varsigma_2, 0) = 1 \quad (16)$$

The fluid inlet and outlet temperatures for the two beds connected in each other are related by the equations

$$\vartheta_1(\xi_1 = 0) = \vartheta_2(\xi_2 = \Lambda), \quad \vartheta_2(\xi_2 = 0) = \vartheta_1(\xi_1 = \Lambda) \quad (17)$$

The effectiveness of the heat exchange of the system can be defined as the heat transferred from storage to another divided by the maximum possible heat to be transferred. The thermal effectiveness can be expressed as

$$\varepsilon = \frac{\dot{C}_f}{C_f + C_m}\int_0^t (\vartheta_{\xi_1=0} - \vartheta_{\xi_1=\Lambda})\,dt \quad (18)$$

3.1. Exact solution

The series connection of the containers (Fig. 1) is analogous to an infinite number of containers connected in series, if the space co-ordinate is understood to continue continuously around the coupled container system. The initial temperature distribution of this analogy is illustrated in Fig. 2. The initial temperature distribution as well as the temperature distribution after start is periodic with respect to the continuous space co-ordinate. Exact solution can be found by applying the Laplace transform also with respect to the space variable ξ corresponding transform variable p. The solution for the twice transformed fluid temperature in the containers becomes

$$\bar{\vartheta} = [\bar{h}(s) + \gamma s/(Bi(1 + \Gamma))]/[p + \bar{h}(s) + \gamma s/(Bi(1 + \Gamma))] \quad (19)$$

The inverse to the time space can be found by using the calculus of residues. The periodicity of the temperature distribution with respect to the place co-ordinate ξ makes it possible to perform the inverse to the ξ-space straightforwardly. The initial temperature distribution can be presented as the Fourier series

$$\theta(\xi, 0, x) = \frac{1}{2} + \frac{2}{\pi}\sum_{k=1}^{\infty}\frac{1}{2k-1}\sin[(2k-1)\pi\xi/\Lambda] \quad (20)$$

The response to sinusoidal initial temperature distribution is also sinusoidal. The amplitude and phase lag of the response is simply found by replacing p with $\mathrm{i}\omega$, where i is imaginary unit and $\omega = \pi/\Lambda$, in the transformed solution. Then the response of the initial temperature distribution of the system of two fixed beds is found by summing up the responses to each term of the Fourier series, Eq. (20). The result for the fluid temperature is

$$\vartheta = \frac{1}{2} + \frac{2}{\pi}\sum_{k=1}^{\infty}\frac{1}{2k-1}\sqrt{[\Re(F_k)]^2 + [\Im(F_k)]^2}\sin\{\omega_k\xi + \arctan[\Im(F_k)/\Re(F_k)]\} \quad (21)$$

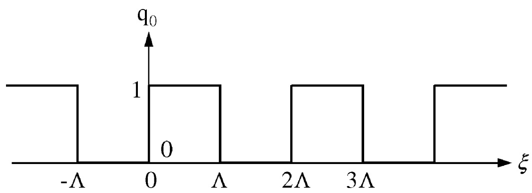

Fig. 2. Presentation of the initial temperature distribution of two coupled fixed bed as an infinite number of fixed beds in series.

The function F_k is

$$F_k = \sum_{n=1}^{\infty} \frac{1}{\mu_n} \frac{\gamma_c \mu_n^2 - \bar{h}(-\mu_n^2)}{\gamma_c + \bar{h}'(-\mu_n^2)} e^{-\mu_n^2 Fo} \quad (22)$$

where $\bar{h}' = d\bar{h}/ds$. The eigenvalues μ_n $(s_n = -\mu_n^2)$ are roots of the equation

$$i\omega_k + \bar{h}(-\mu_n^2) - \gamma\mu_n^2/[Bi(1+\Gamma)] = 0 \quad (23)$$

where $\omega_k = (2k-1)\omega$. This equation can be separated into two equations to determine the real and imaginary parts. The effectiveness of the heat recovery becomes by Eq. (18)

$$\varepsilon = \frac{1}{2} - \frac{4Bi(1+\Gamma)}{\pi\Lambda(1+\gamma)} \sum_{k=1}^{\infty} \frac{1}{2k-1} \times \sum_{n=1}^{\infty} \Im\left(\frac{1}{\mu_n^4} \frac{Bi(1+\Gamma)\bar{h}(-\mu_n^2) - \gamma\mu_n^2}{Bi(1+\Gamma)\bar{h}'(-\mu_n^2) + \gamma} e^{-\mu_n^2 Fo} \right) \quad (24)$$

3.2. Approximate solution

The transformed fluid inlet and outlet temperatures can readily be solved

$$\bar{\vartheta}_{\xi_1=0} = \bar{\vartheta}_{\xi_2=\Lambda} = 1/[s(1+e^{-\bar{h}_*(s)\Lambda})],$$
$$\bar{\vartheta}_{\xi_2=0} = \bar{\vartheta}_{\xi_1=\Lambda} = e^{-\bar{h}_*(s)\Lambda}/[s(1+e^{-\bar{h}_*(s)\Lambda})] \quad (25)$$

The transformed fluid temperature becomes

$$\bar{\vartheta}_1 = \frac{1}{s} \frac{e^{-\bar{h}_*(s)\xi_1}}{1+e^{-\bar{h}_*(s)\Lambda}} = \frac{1}{s} e^{-\bar{h}_*(s)\xi_1} \left(1 + \sum_{n=1}^{\infty} (-1)^n e^{-\bar{h}_*(s)n\Lambda}\right) \quad (26)$$

The inverse transform is

$$\vartheta = \sum_{n=0}^{N} G(A(\xi_1 + n\Lambda), \mu_1^2[Fo - B(\xi_1 + n\Lambda)])U(Fo - B(\xi_1 + n\Lambda)) \quad (27)$$

where $A = K_1\mu_1^2/[Bi(1+\Gamma)]$, $B = (1 - K_1 + \gamma)/[Bi(1+\Gamma)]$. The transformed effectiveness becomes

$$\bar{\varepsilon} = \frac{Bi(1+\Gamma)}{\Lambda(1+\gamma)} \frac{1}{s^2} \frac{1-e^{-\bar{h}_*(s)\Lambda}}{1+e^{-\bar{h}_*(s)\Lambda}} = \frac{Bi(1+\Gamma)}{\Lambda(1+\gamma)} \left[\frac{1}{s^2} + \frac{2}{s^2} \sum_{n=1}^{\infty} (-1)^n e^{-\bar{h}_*(s)n\Lambda}\right] \quad (28)$$

The effectiveness is found as the inverse transform

$$\varepsilon = \frac{Bi(1+\Gamma)}{\Lambda(1+\gamma)} \left(Fo + 2\sum_{n=1}^{\infty} (-1)^n \frac{1}{\mu_1^2} G_1(An\Lambda, \mu_1^2[Fo - Bn\Lambda])U(Fo - Bn\Lambda) \right) \quad (29)$$

3.3. Lumped analysis

The heat conduction resistance of the solids can approximately be combined to the surface heat transfer resistance and the effective heat transfer coefficient becomes $h_e = h/(1+2\phi Bi)$ [15]. Then the equations describing the heat transfer are reduced to the lumped equations for the fluid and solids

$$-\frac{\partial\vartheta}{\partial\xi_e} = \vartheta - \theta + \gamma\frac{\partial\vartheta}{\partial\eta}, \quad \vartheta - \theta = \frac{\partial\theta}{\partial\eta} \quad (30)$$

By applying the Laplace transform with respect to dimensionless time η, we obtain

$$-\frac{d\bar{\vartheta}}{d\xi_e} = \bar{\vartheta} - \bar{\theta} + \gamma s\bar{\vartheta}, \quad \bar{\vartheta} - \bar{\theta} = s\bar{\theta} \quad (31)$$

The solution of the transformed fluid temperature for storage 1 is

$$\bar{\vartheta} = \frac{1}{s} \frac{\exp\{-[s/(1+s) + \gamma s]\xi_e\}}{1 + \exp\{-[s/(1+s)+\gamma s]\Lambda_e\}} = \frac{1}{s} \sum_{n=0}^{\infty} (-1)^n \exp\{-[s/(1+s)+\gamma s](\xi_e + n\Lambda_e)\} \quad (32)$$

The inverse transform is

$$\vartheta = \sum_{n=0}^{\infty} (-1)^n G(\xi_e + n\Lambda, \eta - \gamma\xi_e - \gamma n\Lambda)U(\eta - \gamma\xi_e - \gamma n\Lambda_e) \quad (33)$$

The temperature distribution in the container 2 is obtained from the symmetry relation $\vartheta_2(\xi_{e2}, \eta) = 1 - \vartheta_1(\xi_{e1}, \eta)$. The thermal effectiveness becomes in this case

$$\varepsilon = \frac{1}{\Lambda_e(1+\gamma)} \left(\eta + 2\sum_{n=1}^{\infty} (-1)^n G_1(n\Lambda_e, \eta - n\gamma\Lambda_e)U(\eta - n\gamma\Lambda_e) \right) \quad (34)$$

An alternative solution can be found by applying the Laplace transform, Eq. (4), to Eqs. (31) in addition to the time also with respect to space variable ξ_e. The doubly transformed temperatures of fluid and solids become

$$\bar{\vartheta} = \frac{1+\gamma+\gamma s}{p + (\gamma+p+1)s + \gamma s^2}\theta_{0p},$$
$$\bar{\theta} = \left(\frac{1+\gamma+\gamma s}{p + (\gamma+p+1)s + \gamma s^2} + 1\right)\frac{\theta_{0p}}{1+s} \quad (35)$$

The inverse to time space is obtained by using the calculus of residues. The response to sinusoidal initial temperature distribution is simply found by replacing p with $i\omega$, where i is the imaginary unit and $\omega = \pi/\Lambda_e$.

Again the response of the real initial temperature distribution is found by presenting the distribution as Fourier series and by summing up the responses to each term. The result for fluid temperature is the same form as Eq. (21), but now the functions F_k are defined by

$$F_k = \sum_{n=1}^{2} \frac{1+\gamma+\gamma s_n}{\gamma + \mathrm{i}\omega_k + 2\gamma s_n + 1} \exp(s_n \eta) \tag{36}$$

where the roots s_1 and s_2 are

$$s_{1,2} = -\left[1+\gamma+\mathrm{i}\omega_k \pm \sqrt{(1+\gamma+\mathrm{i}\omega_k)^2 - 4\gamma \mathrm{i}\omega_k}\right] \Big/ (2\gamma) \tag{37}$$

The thermal effectiveness becomes

$$\varepsilon = \frac{1}{2} - \frac{4}{\pi \Lambda_{\mathrm{e}}(1+\gamma)} \sum_{k=1}^{\infty} \frac{1}{2k-1} \times \sum_{n=1}^{2} \Im\left(\frac{1+\gamma+\gamma s_n}{1+\gamma+\mathrm{i}\omega_k + 2\gamma s_n} \frac{\exp(s_n\eta)}{s_n} \right) \tag{38}$$

For gases $\gamma \approx 0$. In the special case $\gamma = 0$, there is one root only. Then the solutions are simplified into

$$\theta = \frac{1}{2} + \frac{2}{\pi} \sum_{n=1}^{\infty} \frac{1}{2n-1} \times \exp\left(-\frac{\omega_n^2}{1+\omega_n^2}\eta\right) \sin\left(\omega_n \xi_{\mathrm{e}} - \frac{\omega_n}{1+\omega_n^2}\eta\right) \tag{39}$$

$$\vartheta = \frac{1}{2} + \frac{2}{\pi} \sum_{n=1}^{\infty} \frac{1}{(2n-1)\sqrt{1+\omega_n^2}} \times \exp\left(-\frac{\omega_n^2}{1+\omega_n^2}\eta\right) \sin\left(\omega_n \xi_{\mathrm{e}} - \frac{\omega_n}{1+\omega_n^2}\eta - \arctan\omega_n\right) \tag{40}$$

$$\varepsilon = \frac{1}{2} - \frac{4}{\pi^2} \sum_{n=1}^{\infty} \frac{1}{(2n-1)^2} \times \exp\left(-\frac{\omega_n^2}{1+\omega_n^2}\eta\right) \cos\left(\frac{\omega_n}{1+\omega_n^2}\eta\right) \tag{41}$$

4. Discussion

The solutions defined by Eqs. (39)–(41) are of similar form as the solutions of parallel flow regenerator [15], but the time and space co-ordinates and gas and solid temperatures both have been exchanged, since the phenomena are analogous and described by similar partial differential equations with identical boundary conditions. The physical problem is, however, completely different.

If the elements consist of bottles containing liquid the lumped analysis is more adequate, but then instead of the heat conduction the effect of internal convection should be combined with the surface heat transfer coefficient. If gas is used as the heat carrier, the thermal resistance is, however, on the gas side and as an approximation the internal resistance can be neglected. The increase of the effective heat conductivity of a spherical droplet due to internal convection has been studied [16].

Heat and mass transfer are analogous and the equations of the same form can frequently be used for both phenomena. Thus, practical applications might be found in mass transfer operations as well. One application could be the damping of concentration oscillations in fluid flow in analogy to the damping of fluid temperature described in the following. A sinusoidal fluid temperature flowing into a solid heat storage can be damped completely when the a part of the fluid flow is bypassed and mixed with the fluid coming from the heat storage [17] as shown in Fig. 3. Using Eq. (10), we obtain the dimensionless heat transfer area Λ and mixing ratio α for complete damping of cyclic inlet fluid temperature $\vartheta = \sin(\omega Fo)$

$$\Lambda = \pi / \{\Im[\bar{h}(\mathrm{i}\omega)] + \gamma\omega/[Bi(1+\Gamma)]\} \tag{42}$$

$$\alpha = \exp(-\Re[\bar{h}(\mathrm{i}\omega)]\pi / \{\Im\bar{h}(\mathrm{i}\omega)\} + \gamma\omega/[Bi(1+\Gamma)]\}) \tag{43}$$

The different solutions are compared in Table 1. It can be seen that the lumped analysis gives a good accuracy. The values in the cases c and d are naturally the

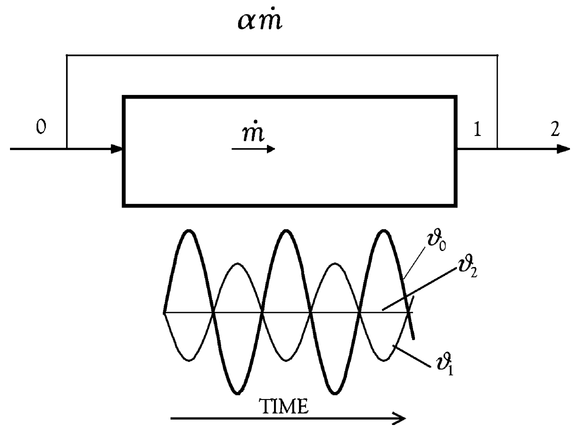

Fig. 3. Fluid temperature damper.

Table 1
Comparison of calculated thermal effectiveness ε calculated by different formulas in the case $\Gamma = 0$ (plates), $Bi = 1$, $Fo = 20$ and $\Lambda = 20$ then $\eta = 15$, $\Lambda_e = 15$

Case	a	b	c	d
$\gamma = 0$	0.716	0.713	0.713	0.713
$\gamma = 0.1$	0.736	0.733	0.733	0.733

(a) Exact solution Eq. (24), (b) approximate solution Eq. (29), (c) lumped exact solution Eq. (34) and (d) lumped exact solution Eq. (38) or Eq. (41).

same, since the solutions, Eqs. (34) and (38), are identical, even their appearance is very different.

The temperature distributions of solids after circulation of fluid between two fixed beds has been started are shown in Fig. 4. It can be seen that heat is transferred from fixed bed 1 to 2, but that if the circulation is continued too long some of the heat already transferred is coming back. This is seen, when the temperature distributions at dimensionless times $\eta = 10$ and $\eta = 14$ (thin line) are compared.

A clear maximum can be seen in the curves for thermal effectiveness of heat recovery in Figs. 5 and 6. It is also seen that as the system size becomes large (Λ_e increases) higher thermal effectiveness for the heat recovery is achieved. An approximation for the maximum can be obtained by differentiating Eq. (29). By taking into account only the first term in the summation we get $G(A\Lambda, \mu_1^2(Fo - B\Lambda)) \approx 0.5$. $G(x, y) \approx 0.5$, when $x \approx y$ and x is large. Then we get for the optimum dimensionless time for heat recovery for large values of Λ

$$Fo_{opt} \approx \Lambda(1 + \gamma)/[Bi(1 + \Gamma)] \tag{44}$$

In the same way, the lumped equation, Eq. (34), gives $\eta_{opt} \approx (1 + \gamma)\Lambda_e$. By using only the first term of the lumped solution, Eq. (41), for gases ($\gamma \approx 0$), we get

$$\eta_{opt} \approx (\Lambda_e/\pi + \pi/\Lambda_e)[\pi - \arctan(\pi/\Lambda_e)] \tag{45}$$

for the optimum dimensionless time for heat recovery.

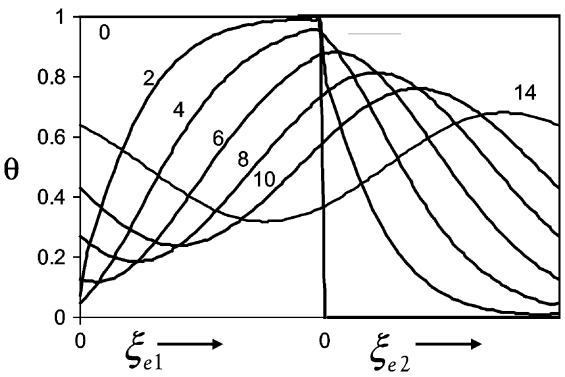

Fig. 4. Temperature distributions of solids in two fixed beds coupled by fluid flow as function of dimensionless space coordinate at different dimensionless times η ($\Lambda_{e1} = \Lambda_{e1} = 10$, $\gamma = 0$).

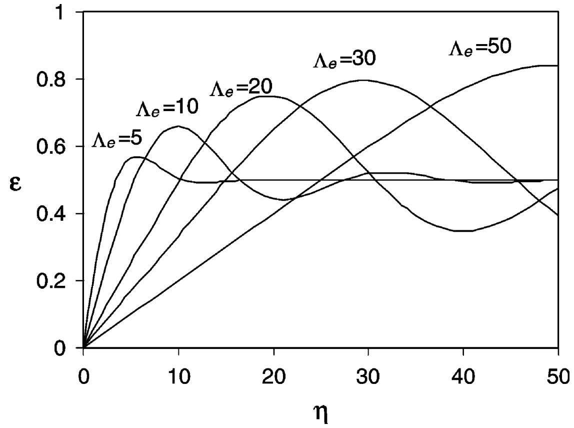

Fig. 5. Thermal effectiveness for heat exchange between two fixed beds coupled by fluid flow ($\gamma = 0$) with different dimensionless heat transfer area Λ_e.

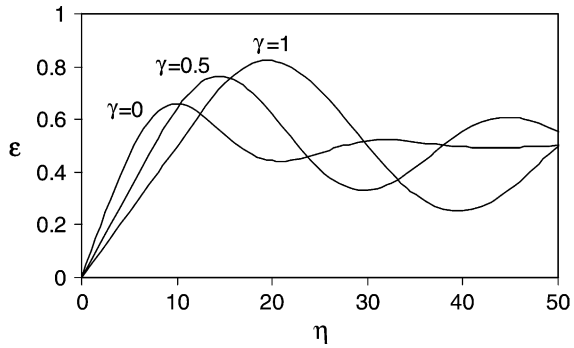

Fig. 6. Thermal effectiveness for heat exchange between two fixed beds ($\Lambda_e = 10$) coupled by fluid flow for heat carriers with different values of γ.

Appendix A

A number of different forms for the functions $G(x, y)$ and related functions have been presented in the literature [1–4,17–22]. In the following a new form in which this function is expressed as a sum of standard Laguerre polynomial is presented. This is in some cases advantageous, since the well-known properties of Laguerre polynomials [23] give possibility to derive different kinds of useful recurrence and other relations for $G(x,y)$ and related functions. Also this solution can be expressed by a single summation instead of the usual double summation, which is computationally advantageous. The required inversion formulas for Laplace transforms are briefly derived. The generating function for Laguerre polynomials $L_n^{(\alpha)}(x)$ is [23]

$$(1-z)^{-\alpha-1}\exp\left(\frac{xz}{z-1}\right)=\sum_{n=0}^{\infty}L_n^{(\alpha)}(x)z^n \tag{A.1}$$

By replacing z with $-1/s$ and by using the inverse transforms term by term to powers of $1/s$, we obtain the inverse transforms (denoted by L^{-1})

$$L^{-1}\{\exp[-xs/(1+s)]/s^{1+n}\}=G_n(x,y),$$
$$L^{-1}\{\exp[-xs/(1+s)]/[s(1+s)]\}=1-G(y,x) \tag{A.2}$$

where $G(x,y)=G_0(x,y)$,

$$G_0(x,y)=\mathrm{e}^{-x}\sum_{n=1}^{\infty}\frac{g_n(x)y^n}{n!},$$
$$G_{k+1}(x,y)=\int_0^y G_k(x,y)\,\mathrm{d}y=\mathrm{e}^{-x}\sum_{n=1}^{\infty}\frac{g_n(x)y^{n+k}}{(n+k)!} \tag{A.3}$$

$g_0(x)=1$, $g_1(x)=x$. The functions $g_n(x)$ are related to Laquerre polynomials $g_n(x)=(-1)^{n+1}xL_n^1(x)/n$, when $n>0$. The values of the polynomials for $n>1$ are rapidly calculated from the recurrence relation

$$g_{n+1}(x)=[(x-2n)g_n(x)+(1-n)g_{n-1}(x)]/(1+n) \tag{A.4}$$

which can be derived from the properties of the Laguerre polynomials. Also useful properties for functions $G_n(x,y)$ can be derived from the properties of Laguerre polynomials. The properties of the functions of the type of $G_n(x,y)$ have been discussed [21,22]. The number of terms required to reach an acceptable truncation error $|z_n|$ can be estimated. By applying the Stirling's formula and the asymptotic expression [24]

$$L_n^{\alpha}(x)=\frac{1}{\sqrt{\pi}}\mathrm{e}^{x/2}n^{\alpha/2-1/4}x^{-\alpha/2-1/4}\cos\left(2\sqrt{\pi nx}-\frac{\alpha\pi}{2}-\frac{\pi}{4}\right) \tag{A.5}$$

for large n we get the asymptotic expression

$$z_n=\mathrm{e}^{-x}g_n(x)\frac{y^n}{n!}$$
$$\propto\frac{(-1)^{n+1}(n-1)^{1/4}x^{1/4}}{2^{1/2}\pi n^{3/2}\mathrm{e}^{x/2}}\left(\frac{ey}{n}\right)^n\cos(2\sqrt{(n-1)x}-3\pi/4) \tag{A.6}$$

By noticing that $|\cos(2\sqrt{(n-1)x}-3\pi/4)|<1$ and $|x^{1/4}\mathrm{e}^{-x/2}|<(2e)^{-1/4}$ it can be concluded that the relation

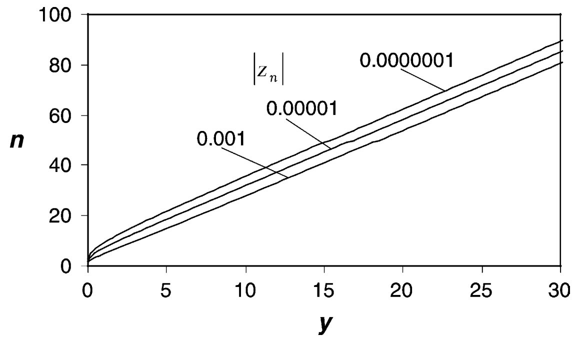

Fig. 7. Number of terms required to reach truncation error $|z_n|$.

$$y<(n/e)\exp[\ln(2^{3/4}\mathrm{e}^{1/2}\pi n^{5/4}|z_n|)/n] \tag{A.7}$$

holds between the maximum value of the variable y and the number n of summation terms used in order to reach required truncation error $|z_n|$. The required number or terms is shown in Fig. 7. Useful approximations for $G(x,y)$ with large values of x and y have been presented [5]. To evaluate the function $G_1(x,y)$ the following approximation

$$G_1(x,y)\approx\frac{1}{2}\mathrm{erfc}\left(\sqrt{x}-\sqrt{y}-\frac{1}{8\sqrt{x}}-\frac{1}{8\sqrt{y}}\right)$$
$$+\mathrm{e}^{-x-y}[xI_0(2\sqrt{xy})+\sqrt{xy}I_1(2\sqrt{xy})] \tag{A.8}$$

when $x>4$ and $y>4$ is useful. Polynomial approximations for the complementary error function *erfc* and modified Bessel functions I of the first kind have been published [23].

References

[1] A. Anzelius, Über erwärmung vermittels durchströmender medien, Z. Angew. Math. Mech. 6 (1926) 291–294.
[2] W. Nusselt, Die theorie des winderhitzers, Z. Ver. Deut. Ing. 71 (1927) 85–91.
[3] T.E.W. Schumann, Heat transfer: a liquid flowing through a porous prism, J. Franklin Inst. 208 (1929) 405–416.
[4] M. Jakob, Heat Transfer, vol. II, Wiley, New York, 1957, pp. 261–341.
[5] F.W. Schmidt, A.J. Willmott, Thermal Energy Storage and Regeneration, McGraw-Hill, New York, 1981.
[6] M. Riaz, Analytical solutions for single- and two-phase models of packed-bed thermal storage systems, ASME J. Heat Transfer 99 (1977) 489–492.
[7] A.E. Saez, B.J. McCoy, Transient analysis of packed bed thermal storage systems, Int. J. Heat Mass Transfer 26 (1983) 49–54.
[8] D. Handley, P.J. Heggs, The effect of thermal conductivity of the packing material on transient heat transfer in a fixed bed, Int. J. Heat Mass Transfer 12 (1969) 549–570.

[9] N. Amundson, Solid fluid interactions in fixed and moving beds, Ind. Eng. Chem. 48 (1956) 26–43.

[10] F.W. Schmidt, J. Szego, Transient response of solid sensible heat thermal storage units-single fluid, ASME J. Heat Transfer 100 (1978) 737–746.

[11] D.J. Gunn, P.V. Narayanan, Axial thermal dispersion and particle to fluid transfer in packed-fluidized beds, Int. J. Heat Mass Transfer 24 (1981) 1405–1411.

[12] W.A. Sirignano, Linear model for convective heat transfer in a spray, in: C. Casci (Ed.), Recent Advances in the Aerospace Sciences, Springer Verlag, 1985, pp. 213–236.

[13] H.S. Carslaw, J.C. Jaeger, Conduction of Heat in Solids, Oxford University Press, Oxford, UK, 1959.

[14] M.D. Mikhailov, M.N. Özişik, Unified Analysis and Solutions of Heat and Mass Diffusion, Dover Publications, New York, 1984.

[15] H. Hausen, Wärmeübertragung im Gegenstrom, Gleichstrom und Kreuzstrom, Springer-Verlag, Berlin, 1976, pp. 259–429.

[16] B. Abramzon, W.A. Sirignano, Droplet vaporization model for spray combustion calculations, Int. J. Heat Mass Transfer 32 (1989) 1605–1618.

[17] J.J. Saastamoinen, Heat transfer in crossflow regenerators, Int. J. Heat Mass Transfer 42 (1999) 3201–3212.

[18] B.S. Baclic, P.J. Heggs, On the search for new solutions of the single-pass crossflow heat exchanger problem, Int. J. Heat Mass Transfer 28 (1985) 1965–1976.

[19] C.-H. Li, A new simplified formula for crossflow heat exchanger effectiveness, ASME J. Heat Transfer 109 (1987) 521–522.

[20] A. Montakhab, Convective heat transfer in porous media, ASME J. Heat Transfer 101 (1979) 507–510.

[21] J. Łach, W. Pieczka, On the properties of some special functions related to Bessel's functions and their application in heat exchanger theory, Int. J. Heat Mass Transfer 27 (1984) 2225–2238.

[22] F.E. Romie, Two functions used in the analysis of crossflow exchangers, regenerators, and related equipment, ASME J. Heat Transfer 109 (1987) 518–521.

[23] M. Abramowitz, I. Stegun, Handbook of Mathematical Functions, Dover Publications, New York, 1972, pp. 782–784.

[24] N.N. Lebedev, Special Functions and Their Applications, Dover Publications, New York, 1972, p. 87.